



High-density EEG coherence analysis using functional units applied to mental fatigue

Michael ten Caat^{a,b}, Monique M. Lorist^{b,c}, Eniko Bezdan^c,
Jos B.T.M. Roerdink^{a,b,*}, Natasha M. Maurits^{b,d}

^a Institute for Mathematics and Computing Science, University of Groningen, The Netherlands

^b BCN Neuroimaging Center, University Medical Center Groningen, University of Groningen, The Netherlands

^c Experimental and Work Psychology, University of Groningen, The Netherlands

^d Department of Neurology, University Medical Center Groningen, University of Groningen, The Netherlands

ARTICLE INFO

Article history:

Received 11 December 2007

Received in revised form 26 March 2008

Accepted 28 March 2008

Keywords:

Multichannel EEG visualization

Coherence analysis

Mental fatigue

ABSTRACT

Electroencephalography (EEG) coherence provides a quantitative measure of functional brain connectivity which is calculated between pairs of signals as a function of frequency. Without hypotheses, traditional coherence analysis would be cumbersome for high-density EEG which employs a large number of electrodes. One problem is to find the most relevant regions and coherences between those regions in individuals and groups. Therefore, we previously developed a data-driven approach for individual as well as group analyses of high-density EEG coherence. Its data-driven regions of interest (ROIs) are referred to as functional units (FUs) and are defined as spatially connected sets of electrodes that record pairwise significantly coherent signals. Here, we apply our data-driven approach to a case study of mental fatigue. We show that our approach overcomes the severe limitations of conventional hypothesis-driven methods which depend on previous investigations and leads to a selection of coherences of interest taking full advantage of the recordings under investigation. The presented visualization of (group) FU maps provides a very economical data summary of extensive experimental results, which otherwise would be very difficult and time-consuming to assess. Our approach leads to an FU selection which may serve as a basis for subsequent conventional quantitative analysis; thus it complements rather than replaces the hypothesis-driven approach.

© 2008 Elsevier B.V. All rights reserved.

1. Introduction

A functional relationship between different brain regions is generally associated with synchronous electrical activity in these regions (Varela et al., 2001). Higher-level cognitive mechanisms are associated with activity at lower frequencies and more global synchronization; lower-level mechanisms are associated with activity at higher frequencies and more local synchronization (Nunez et al., 1997; von Stein and Sarnthein, 2000). Electroencephalography (EEG) coherence between signals recorded from pairs of electrodes as a function of frequency might be used as a quantitative measure for this synchrony (Halliday et al., 1995).

EEG coherence is usually visualized as a two-dimensional graph layout. Vertices (drawn as dots) represent electrodes and edges (drawn as lines between dots) represent significant coherences between electrode signals. For high-density EEG, this layout may suffer from a large number of overlapping edges, resulting in visual clutter (Kamiński et al., 1997; Stein et al., 1999). Regarding the analysis of high-density EEG coherence, one problem is to find the most relevant regions (groups of electrodes) and the most relevant coherences between those regions. Another problem is to compare coherences of interest across groups.

One common approach for coherence analysis is the data-driven approach. This method does not provide any spatial information; it assigns a quantity to a coherence graph as a whole. Popular examples of such quantities are cluster index (level of clustering) and characteristic path length (average path length) (Achard et al., 2006; Salvador et al., 2005; Sporns, 2002; Watts and Strogatz, 1998). A graph with a high cluster index in combination with a low characteristic path length is said to reflect small-world properties. Although a high cluster index is related to a global organization of local units (i.e., clusters, which may here be interpreted as EEG

* Corresponding author at: Institute for Mathematics and Computing Science, University of Groningen, Nijenborgh 9, 9747 AG Groningen, The Netherlands. Tel.: +31 50 3633931; fax: +31 50 3633800.

E-mail addresses: mtc@cs.rug.nl (M. ten Caat), m.m.lorist@rug.nl (M.M. Lorist), j.b.t.m.roerdink@rug.nl (J.B.T.M. Roerdink), n.m.maurits@neuro.umcg.nl (N.M. Maurits).

sources), it does not provide information on the size or number of those units (Sporns, 2002), nor on their location. The other quantities do not provide this information either.

Another common approach for EEG coherence analysis is the hypothesis-driven approach. This usually makes a regular subselection of the available coherences (Maurits et al., 2006), because coherence analysis of all electrode pairs would be cumbersome for high-density EEG. A major drawback of this approach is that the majority of the coherences is ignored.

We earlier presented a method for data-driven region of interest (ROI) detection taking into account spatial properties (ten Caat et al., 2007b, c, 2008). The data-driven ROIs were referred to as *functional units* (FUs) and were defined as spatially connected sets of electrodes recording pairwise significantly coherent signals. For individual datasets, FUs are displayed in a so-called *FU map* which preserves electrode locations. An FU map visualizes the size and location of all FUs, and connects FUs if the average coherence between them exceeds a threshold (ten Caat et al., 2007b, c, 2008).

Because there is much variation between individual FU maps, we additionally proposed two types of *group analysis* (ten Caat et al., 2008). First, the *group mean coherence map*, which preserves dominant features from a collection of individual FU maps. Second, the *group FU size map*, which visualizes the average FU size per electrode across a collection of individual FU maps.

In this paper, our data-driven method for individual and group coherence analysis is applied in a mental fatigue study. We indicate how the data-driven method leads to an FU selection, which may serve as a basis for subsequent conventional quantitative analysis. The latter will not be discussed here.

2. Methods

2.1. Participants and task

Brain responses were recorded from a group of five healthy participants (three women) between 19 and 24 years of age, using an EEG cap with 59 scalp electrodes (Fig. 1). A task switching paradigm (Lorist et al., 2000) was used, which allows to study the effect of mental fatigue on cognitive control processes involved in the planning and preparation for future actions (Lorist et al., 2000). Mental fatigue refers to the effects that people may experience after or

during prolonged periods of demanding cognitive activity and was induced here by 2 h of continuous task performance, that is by time on task (Lorist et al., 2000, 2005). During task execution subjects were facing a color monitor on which a square (4 × 4 cm) subdivided into four equal quadrants was displayed. Stimuli were red or blue letters, randomly chosen from the set {A, E, O, U, G, K, M, R}, which were presented in the center of one of the quadrants in a clockwise order, one by one.

Participants were instructed to make either a left or right hand response on each trial by pressing a response button as quickly and accurately as possible. They responded (left/right) to the color (red/blue) of the stimulus if it was presented in one of the two upper quadrants, and to letter identity (vowel/consonant) for one of the two lower quadrants. Thus, subjects switched between the color and letter tasks on every second trial. Therefore, responses to stimuli are so-called switch trials for the upper left and lower right quadrants, and repetition trials for the upper right and lower left quadrants. The time between the response and the next stimulus was randomly chosen to be 150, 600, 1500, or 2400 ms.

The aim of our data-driven approach is to indicate ROIs and coherences of interest between those ROIs when no strong hypotheses can be formulated based on existing evidence. For simplicity, we here restrict the analysis to the condition in which subjects have ample time to prepare for a task switch (i.e., 600 ms response-stimulus interval). The switch task was performed continuously for 120 min, a period which was divided into six blocks of 20 min for subsequent analysis. Because effects of mental fatigue are more pronounced in conditions in which relatively high demands are placed on cognitive control processes, analysis was further restricted to switch trials only (Lorist et al., 2000). To examine the effects of mental fatigue, which increases with time on task, we compared responses from the first and the last 20 min block (blocks 1 and 6). Responses where the subject gave an incorrect answer were disregarded.

2.2. EEG coherence

As a result of volume conduction (Lachaux et al., 1999), multiple electrodes can record a signal from a single source in the brain. Therefore, nearby electrodes usually record similar signals. However, because sources of activity at different locations may be synchronous, electrodes far apart can also record similar signals. A measure for this synchrony is coherence, calculated between pairs of signals as a function of frequency. The coherence c_λ as a function of frequency λ for two continuous time signals x and y is defined as the absolute square of the cross-spectrum f_{xy} normalized by the autospectra f_{xx} and f_{yy} (Halliday et al., 1995), having values in the interval [0, 1]: $c_\lambda(x, y) = |f_{xy}(\lambda)|^2 / f_{xx}(\lambda)f_{yy}(\lambda)$. To calculate the coherence for an event-related potential (ERP) with L repetitive stimuli, the EEG data can be segmented into L segments. A significance threshold ϕ for the estimated coherence is then given by Halliday et al. (1995)

$$\phi = 1 - p^{1/(L-1)}, \quad (1)$$

where p is a probability value associated with a confidence level α ($p = 1 - \alpha$).

The average number of correct responses for the different blocks was around 65, but with a rather large inter-subject variation. Therefore, brain responses for the first 40 trials with a correct response were selected (for each block and each subject at least 40 correct responses were available). Disjoint segments ([-0.1, 0.88] s around the stimulus) were used for further analysis, consisting of responses for 20 trials at each switch. We used an average reference which is suitable for coherence analysis of high-density EEG (Nunez et al., 1997; Maurits et al., 2006), applied

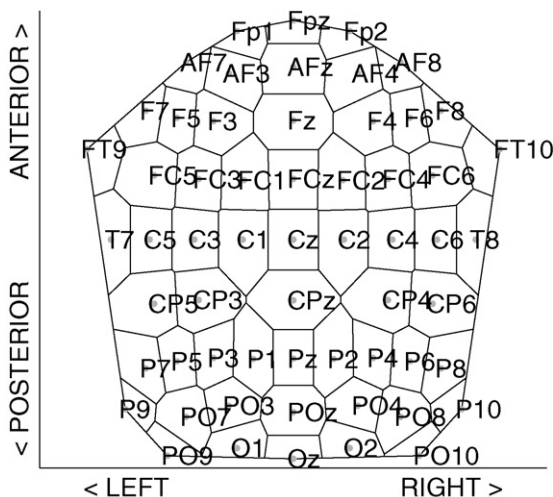


Fig. 1. Voronoi diagram of the electrode positions. To each electrode a 'Voronoi cell' is associated, consisting of all points that are nearest to that electrode. Electrode labels are shown in corresponding cells (top view of the head, nose at the top).

a high-pass filter (0.16 Hz) and a notch filter (50 Hz), and resampled from 500 to 512 Hz (BrainVision Analyzer 1.05, Brain Products GmbH). Then data were transferred to EEGLAB (Delorme and Makeig, 2004), running under Matlab (The MathWorks). A procedure from Neurospec was adopted to compute the coherence (<http://www.neurospec.org>), using a custom-made script to compute coherences between all 1711 pairs of electrode signals. We calculated coherence within the following EEG frequency bands: delta (1–3 Hz), theta (4–7 Hz), alpha (8–12 Hz), beta (13–23 Hz), lower gamma (24–35 Hz), and higher gamma (36–70 Hz). Since conductive gel might accidentally connect two adjacent electrodes and thereby produce very high coherences, coherences higher than 0.99 were ignored between signals corresponding to two neighboring electrodes. The corresponding coherence threshold for $p = 0.01$ and $N = 40$ segments is $\phi = 1 - 0.01^{1/(40-1)} \approx 0.11$.

2.3. Individual analysis: FU map

The data for individual dataset analysis are represented by a *coherence graph* with vertices representing electrodes. Coherences above the significance threshold (Eq. (1)) are represented by edges, coherences below the threshold are ignored. To determine spatial relationships between electrodes, a Voronoi diagram is employed which partitions the plane into regions of points with the same nearest electrode (Fig. 1). The area enclosed by the boundaries of a region is referred to as (Voronoi) cell. We call two cells spatially connected if they have a boundary in common.

Because multiple electrodes can record a signal from a single source, a spatially connected set of electrodes recording similar signals is considered as a data-driven ROI, referred to as FU. More precisely, an FU is represented in the EEG coherence graph by a set of spatially connected vertices which form a ‘clique’, meaning that the coherence between any pair of electrodes in an FU exceeds the significance threshold (ten Caat et al., 2007b, 2008). FU detection is motivated by the assumption that larger FUs correspond to stronger source signals and are therefore more interesting.

Earlier we developed three FU detection methods. One is a maximal clique-based (MCB) method which detects FUs which are as large as possible (ten Caat et al., 2007b, 2008). Its algorithm computes the correct FUs according to the maximal clique definition, but is very time-consuming. Therefore, we developed two alternative approaches. The first is a watershed-based (WB) method which approximates FUs in a greedy way and is faster (ten Caat et al., 2007c). The WB method, originally developed to segment images into objects, was adapted to cluster electrodes into subsets which resemble cliques. Finally, we introduced an improved watershed-based (IWB) method which merges neighboring FUs if their union is a clique in the coherence graph (ten Caat et al., 2008). The IWB method is used here, because it is much faster than the MCB method, and gives a better FU approximation than the WB method (ten Caat et al., 2008).

Given the FUs, the *inter-FU coherence* c'_λ at frequency λ between two FUs, W_1 and W_2 , is defined as the sum of the coherence values between one vertex in W_1 and the other vertex in W_2 , scaled by the maximal number of edges between W_1 and W_2 (ten Caat et al., 2007b):

$$c'_\lambda(W_1, W_2) = \frac{\sum_{i,j} \{c_\lambda(v_i, v_j) | v_i \in W_1, v_j \in W_2\}}{|W_1| \cdot |W_2|}. \quad (2)$$

Here, $|W_i|$ indicates the number of vertices in W_i . Note that coherences between any pair of vertices are taken into account, including those below the threshold.

An *FU map* visualizes each FU as a set of cells with identical gray value, with different gray values for adjacent FUs (e.g., Fig. 2). For visualization, a line is drawn between FU centers if the corresponding inter-FU coherence exceeds a threshold. We consistently choose this threshold to be equal to the significance threshold (Eq. (1)), as we already used this threshold to determine the coherence graph. Because larger FUs are considered to be more interesting (ten Caat et al., 2008), only FUs of at least four cells are considered.

2.4. Group analyses: group mean coherence map and group FU size map

FU maps differ from individual to individual, making group analysis difficult. For this reason we previously introduced two group maps for data-driven group analysis (ten Caat et al., 2008).

First, a *group mean coherence graph* was defined as the graph containing the mean coherence for every electrode pair computed across a group (ten Caat et al., 2008). To obtain a data-driven coherence visualization for a group, only the edges with a value exceeding the coherence threshold (Eq. (1)) are maintained. Next, an FU map, referred to as *group mean coherence map*, is created for this graph.

Second, a *group FU size map* visualizes the average FU size for every electrode across a group, based on the individual FU maps (ten Caat et al., 2008). The average FU size s of an electrode v is computed as

$$s(v) = \sum_{j \in \text{all datasets}} \frac{|FU_j(v)|}{\#\text{datasets}},$$

with $|FU_j(v)|$ the size of the FU containing v for dataset j . The value s for an electrode is mapped to the gray value of its corresponding cell, with lighter gray for higher average FU sizes, similar to a (gray scale) topographic map (ten Caat et al., 2007a). Consequently, a light cell in an FU size map indicates that the corresponding electrode is on average part of large FUs and is therefore more interesting. (Recall that, on the contrary, white cells in FU maps and group mean coherence maps are considered to be the least interesting, because they are not part of sufficiently large FUs.)

To summarize, as a result of the way in which it is calculated, the group mean coherence map displays coherences (and the involved FUs) with a higher mean value. Because this FU map is calculated based on average coherence values between electrode pairs, both very high coherences in a few subjects and coherences which are on average high in many subjects can result in FUs and coherences in the group mean coherence map. The group FU size map emphasizes those electrodes which are often part of a large FU in the individual subjects. It indicates where on average the larger FUs are located.

3. Results

For all results, we set $p = 0.01$, corresponding to a coherence threshold $\phi \approx 0.11$.

3.1. Individual analysis: FU map

Individual FU maps for all participants were created for blocks 1 (non-fatigued, Fig. 2) and 6 (fatigued, Fig. 3). First, we comment on the general interpretation of FU maps before describing the FU maps for this particular case study. Cells within one FU correspond to electrodes whose signals are all (pairwise) significantly coherent. Thus, if one FU covers an area including left and right frontal electrodes (e.g., Fig. 2, participant 1, 8–12 Hz), then all coherences between electrodes in the left and right frontal area are significant. Alternatively, if there are two separate left and right frontal

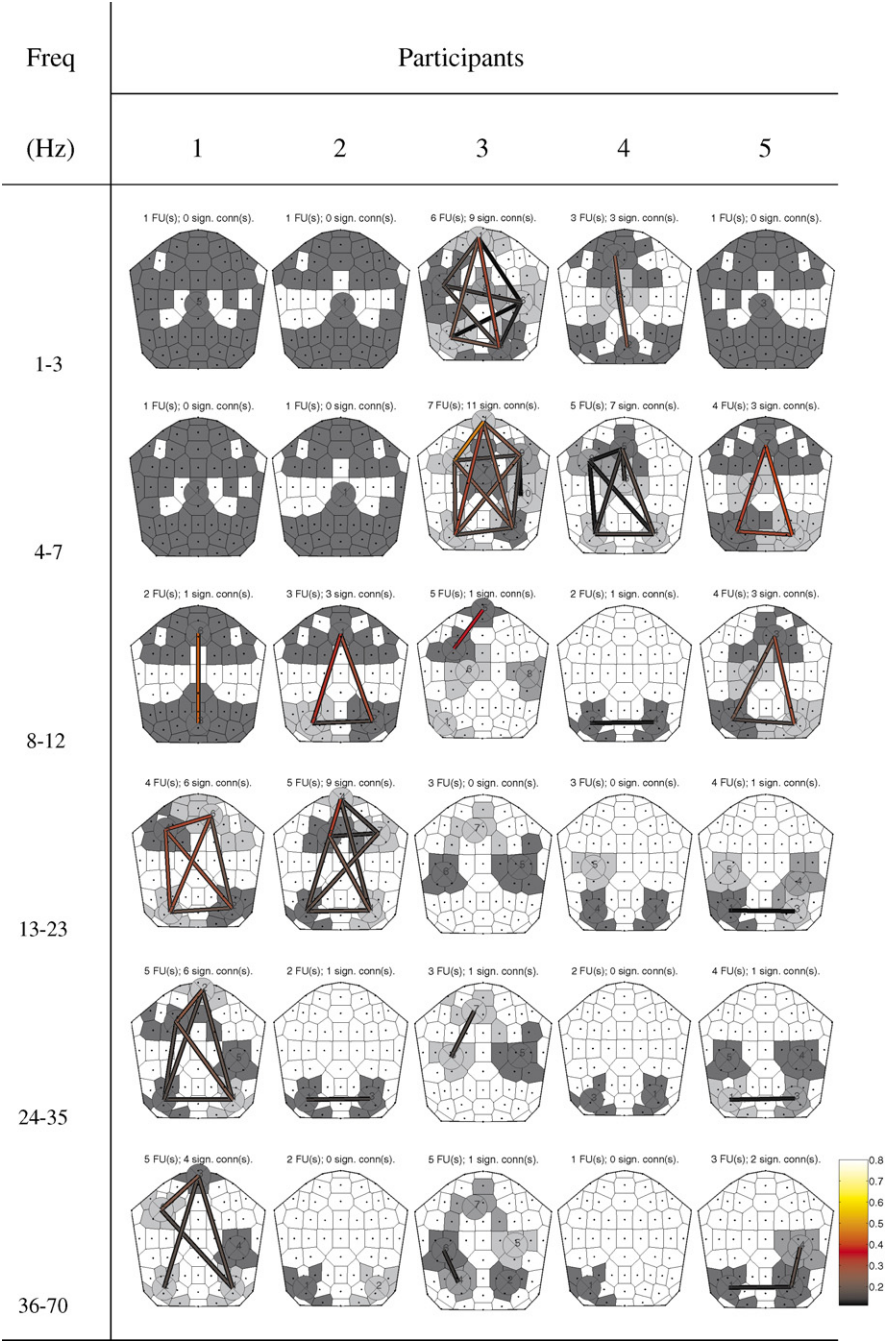


Fig. 2. IndividualFU maps, block 1 (non-fatigued), for each participant (numbered 1–5), with $p = 0.01$ and $|FU| \geq 4$. Each FU is visualized as a set of cells with identical gray value, with different gray values for adjacent FUs. White cells are part of FUs with a size smaller than 4. A line connects FUs if the inter-FU coherence exceeds the significance threshold, with its color depending on the value (see color bar, with minimum corresponding to the coherence threshold $\phi \approx 0.11$ for $p = 0.01$; the color bar is the same for all FU maps). (For interpretation of the references to color in this figure legend, the reader is referred to the web version of the article.)

FUs and they are connected by a line (e.g., Fig. 2, participant 1, 13–23 Hz), then the *average* of all coherences between one electrode in the left and the other electrode in the right frontal FU is significant.

Within a participant, two FU maps from separate blocks are usually highly similar regarding FU locations and connections between FUs. On the contrary, differences between participants are found to be large. Considering the FU maps per participant, FUs are generally largest for the lowest frequencies (both in blocks 1 and 6). Simultaneously, the total number of electrodes in FUs decreases for increasing frequencies in the range 1–35 Hz. Above 35 Hz, this

number does not continue to decrease. Further, the number of significant longer-distance coherences (either within one large FU, or between two smaller FUs) also decreases with increasing frequency.

Overall, the coherence between frontal FUs is significant in the majority of the FU maps. Left and right parieto-occipital FUs, sometimes part of one larger FU, occur in most cases. If frontal FUs and lateral parieto-occipital FUs coexist, then the coherence between those FUs is usually significant and often includes interhemispheric coherences. Further, left and right centroparietal FUs occur regularly. Centrally located FUs are found occasionally.

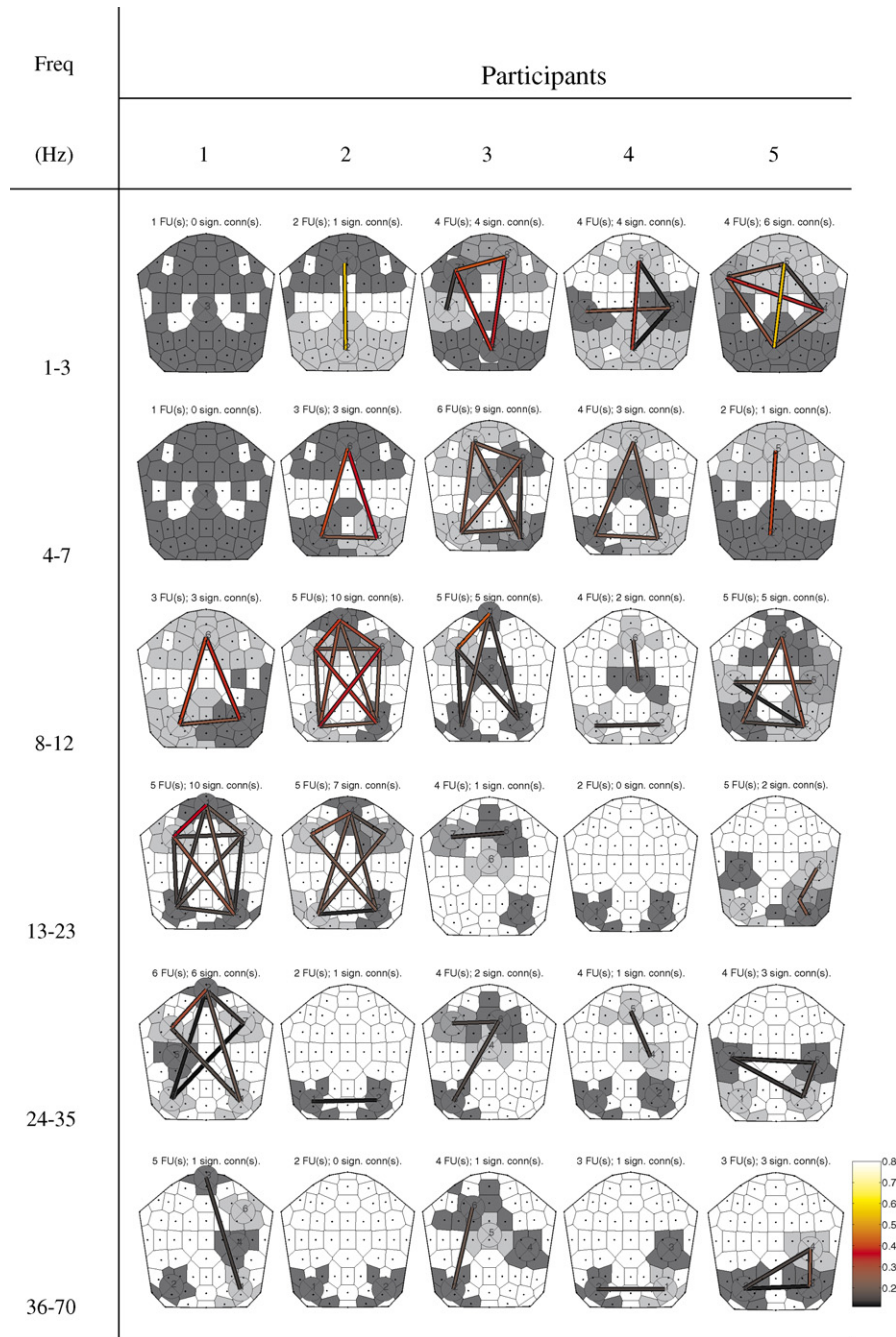


Fig. 3. Individual FU maps, block 6 (fatigued). Same parameters as in Fig. 2. (For interpretation of the references to color in this figure legend, the reader is referred to the web version of the article.)

In summary, differences between participants are generally larger than differences within participants between blocks 1 and 6. Lower frequencies show a more global synchronization, having larger FUs and a larger number of longer-distance coherences between FUs. For higher frequencies, decreasing FU sizes and a reduction of longer-distance coherences indicate a more local synchronization.

3.2. Group analyses: group mean coherence map and group FU size map

The coherence data for block 1 (non-fatigued participants) is put in one group, and for block 6 (the same, fatigued, participants) in another group.

3.2.1. Group mean coherence map

Group mean coherence maps (Fig. 4) were created for block 1 (non-fatigued) and block 6 (fatigued). First, we comment on correspondences between group mean coherence maps and the individual FU maps, and correspondences within the group mean coherence maps between blocks 1 and 6.

As differences within participants are small between blocks 1 and 6, differences in the group mean coherence maps are also small between these two blocks. The largest FUs occur generally for the lowest frequencies (for both the non-fatigued and the fatigued condition). The number of electrodes which are part of an FU and the number of significant longer-distance coherences (either within one large FU, or between two smaller FUs) both decrease with increasing frequency. Further, frontal FUs occur for both blocks 1

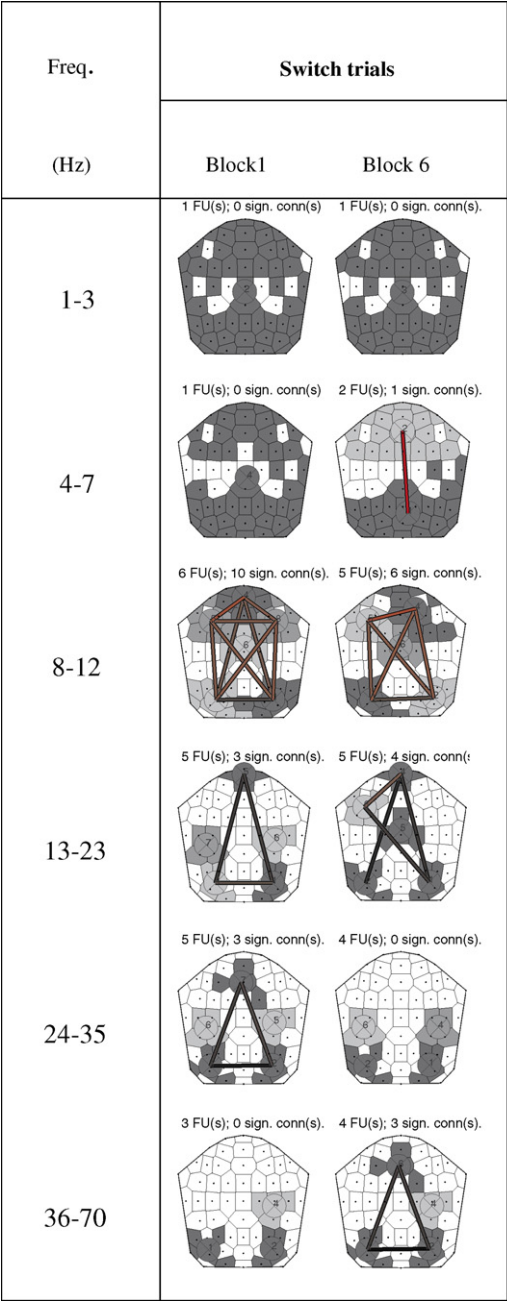


Fig. 4. Group mean coherence maps for block 1 (non-fatigued, left) and block 6 (fatigued, right), with $p = 0.01$ and $|FU| \geq 4$. The line color depends on the inter-FU coherence (see color bar, bottom right, with minimum corresponding to the coherence threshold $\phi \approx 0.11$; the color bar is the same for all FU maps). Above each group mean coherence map, the number of FUs and the number of connecting lines between FUs are displayed. (For interpretation of the references to color in this figure legend, the reader is referred to the web version of the article.)

and 6 in the 1–12 Hz range. For higher frequencies, frontal FUs are smaller (or absent). As most individual FU maps have lateral parieto-occipital FUs, every group mean coherence map also has such FUs. Significant anterior–posterior coherences (between frontal and lateral parieto-occipital FUs) exist within one FU or between two FUs in the 1–23 Hz range for blocks 1 and 6.

Apparent differences in the group mean coherence maps between blocks 1 and 6 occur in the two highest frequency bands (24–35 and 36–70 Hz), with anterior–posterior connections present in one block but absent in the other. Those connections

involve FUs with a size just above the threshold (four cells). Other differences, between individual FU maps and group mean coherence maps, involve central FUs, which are present in block 1 for 8–12 Hz and in block 6 for 8–23 Hz in the group mean coherence maps. Nevertheless, they are not present in the majority of the individual FU maps for the corresponding frequency bands and blocks. However, there is no significant coherence between a central FU and any other FU.

3.2.2. Group FU size map

Group FU size maps were created for all participants for blocks 1 and 6 per frequency band (Fig. 5). Confirming the picture of the individual FU maps and the group mean coherence maps, the max-

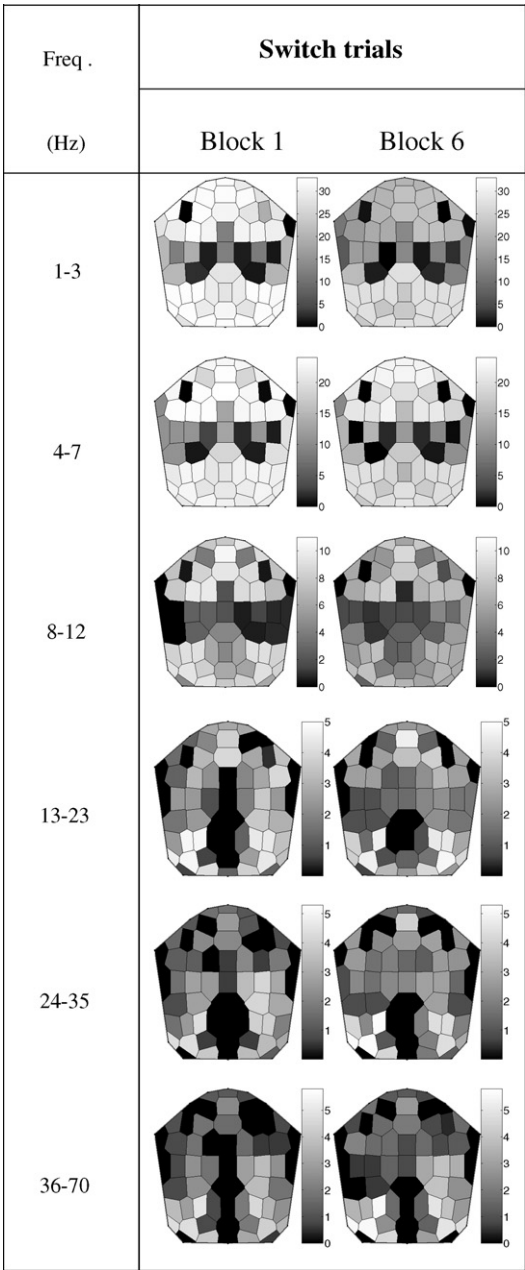


Fig. 5. Group FU size maps for block 1 (non-fatigued, left) and block 6 (fatigued, right). Same parameters as in Fig. 4. The gray scale range is adapted per frequency band (see right bars, with maximum equal to the maximum average FU size). A lighter cell indicates that the corresponding electrode is on average part of a larger FU.

imum average FU size per electrode (cf., ‘color’ bar) decreases with increasing frequency for both blocks 1 and 6 in the frequency range 1–23 Hz; for higher frequencies, the maximum average FU size does not vary much. The maximum average FU size also does not vary much between the two blocks, per frequency band.

The main difference between blocks 1 and 6 occurs for 1–3 Hz. In this frequency band, the highest average FU sizes occur in both anterior and posterior areas for block 1, and in a posterior area for block 6. Further, there are no clear differences between blocks 1 and 6 for higher frequencies. Large FUs are located for 4–7 Hz in frontal and parieto-occipital areas, for 8–12 Hz in frontal areas, and for 13–70 Hz in left and right parieto-occipital areas. The smallest FUs occur for blocks 1 and 6 in similar areas. For 1–7 Hz, the smallest FUs appear in lateral centroparietal areas. For higher frequencies, the smallest FUs are found in central, centroparietal, and occipital areas. Temporal FUs are generally small.

In summary, for a subsequent quantitative analysis, based on the above data-driven FU-map visualizations, we suggest to explore power for and coherences between mid-anterior (AFz or Fz), bilateral frontal (F5 and F6) and bilateral posterior (PO7 and PO8) electrode locations. Particular attention should be paid to coherences between anterior and posterior contralateral electrodes (e.g., F5–PO8). Frequency bands of interest are 1–3, 4–7 and 8–12 Hz, in particular.

4. Discussion and conclusions

Our data-driven method for high-density EEG coherence analysis based on FUs was applied to a case study for which no existing evidence was available to formulate strong hypotheses. In this study, a prolonged switching task was used to induce mental fatigue. We used our approach to suggest electrode pairs and frequency bands of interest for later quantitative power and coherence analysis of this fatiguing task.

Generally speaking, in line with known EEG properties (Nunez et al., 1997; von Stein and Sarnthein, 2000), lower frequencies were associated with a more global synchronization and higher frequencies with a more local one. Accordingly, both the individual FU maps and the group mean coherence maps had larger FUs and more longer-distance inter-FU coherences for lower frequencies. Further, smaller FU sizes and a reduction of longer-distance coherences occurred for higher frequencies. FU map differences were generally large between participants, but small between the non-fatigued and fatigued conditions. These large inter-individual differences are not a property of our analysis, but probably of the underlying data. The data-driven approach we take likely makes these differences more clear than a hypothesis-driven approach in which certain pairs of electrodes are selected beforehand, coherences are calculated and a statistical analysis is applied straightforwardly to assess differences between groups. Improved insight in inter-individual differences and similarities in coherence may therefore be considered an additional advantage of our approach.

Common features of individual FU maps were generally preserved in the group mean coherence maps. Differences between the non-fatigued and fatigued condition appeared in the group FU size maps for the lowest frequency band (1–3 Hz), with the largest FUs located both anteriorly and posteriorly for the non-fatigued group, and posteriorly for the fatigued group. Because mental fatigue is supposed to affect higher-level cognitive processes which are associated with lower EEG frequencies, this may explain why the largest difference between the non-fatigued and fatigued group occurs in the lowest EEG frequency band. Therefore, for subsequent quantitative power and coherence analysis, our group analysis suggests to take anterior and posterior electrodes into account and focus on low frequency bands.

In summary, our method thus specifies the frequency band(s) of interest and intrahemispheric, interhemispheric, and homologous coherences for subsequent quantitative analysis. Additionally, interhemispheric coherences between (left/right) anterior and (right/left) posterior areas were suggested, which have so far not been considered in hypothesis-driven approaches. Our data-driven method suggests that coherences between these electrode pairs may be particularly interesting to detect differences between fatigued and non-fatigued conditions during execution of a cognitive switching task.

To conclude, the presented data-driven method for high-density EEG coherence analysis, employing FU maps and two types of group maps, can be applied to situations for which no strong hypotheses can be formulated based on existing evidence. It overcomes the severe limitations of conventional hypothesis-driven methods which depend on previous measurements and leads to a selection of coherences which takes full advantage of the actual measurement. Our method distinguishes between local coherence (within an FU) and global coherence (between FUs) and results are in line with common EEG knowledge. Our approach can be applied to any coherence data set, but is particularly suited for datasets containing so many electrodes that an exhaustive analysis which considers all possible electrode pairs is no longer feasible (i.e., 20 electrodes, which already leads to 190 possible pairs). Previously, we showed that the analysis is very fast and takes approximately 0.05 s for 128 electrodes (ten Caat et al., 2008), in a study on the effects of ageing on cognitive task performance. Altogether, our visualization of (group) FU maps provides a very economical data summary of a very extensive set of experimental results, which otherwise would be very difficult and time-consuming to assess and which can be used as a guideline for further quantitative analysis.

References

- Achard S, Salvador R, Whitcher B, Suckling J, Bullmore E. A resilient, low-frequency, small-world human brain functional network with highly connected association cortical hubs. *J Neurosci* 2006;26(1):63–72.
- Delorme A, Makeig S. EEGLAB: an open source toolbox for analysis of single-trial EEG dynamics including independent component analysis. *J Neurosci Methods* 2004;134:9–21.
- Halliday DM, Rosenberg JR, Amjad AM, Breeze P, Conway BA, Farmer SF. A framework for the analysis of mixed time series/point process data—theory and application to the study of physiological tremor, single motor unit discharges and electromyograms. *Prog Biophys Mol Biol* 1995;64(2/3):237–78.
- Kamiński M, Blinowska K, Szeleńberger W. Topographic analysis of coherence and propagation of EEG activity during sleep and wakefulness. *Electroencephalogr Clin Neurophysiol* 1997;102:216–27.
- Lachaux JP, Rodriguez E, Martinerie J, Varela FJ. Measuring phase synchrony in brain signals. *Hum Brain Mapp* 1999;8(4):194–208.
- Lorist MM, Klein M, Nieuwenhuis S, de Jong R, Mulder G, Meijman TF. Mental fatigue and task control: planning and preparation. *Psychophysiology* 2000;37:614–25.
- Lorist MM, Boksem MAS, Ridderinkhof KR. Impaired cognitive control and reduced cingulate activity during mental fatigue. *Cogn Brain Res* 2005;24:199–205.
- Maurits NM, Scheeringa R, van der Hoeven JH, de Jong R. EEG coherence obtained from an auditory oddball task increases with age. *J Clin Neurophysiol* 2006;23(5):395–403.
- Nunez PL, Srinivasan R, Westdorp AF, Wijesinghe RS, Tucker DM, Silberstein RB, Cadusch PJ. EEG coherence. I. Statistics, reference electrode, volume conduction, Laplacians, cortical imaging, and interpretation at multiple scales. *Electroencephalogr Clin Neurophysiol* 1997;103(5):499–515.
- Salvador R, Suckling J, Coleman MR, Pickard JD, Menon D, Bullmore E. Neurophysiological architecture of functional magnetic resonance images of human brain. *Cereb Cortex* 2005;15:1332–42.
- Sporns O. Graph theory methods for the analysis of neural connectivity patterns. In: Kötter R, editor. *Neuroscience databases. A practical guide*. Chapter 12: Klüwer; 2002. p. 169–83.
- Stein AV, Rappelsberger P, Sarnthein J, Petsche H. Synchronization between temporal and parietal cortex during multimodal object processing in man. *Cereb Cortex* 1999;9:137–50.
- ten Caat M, Maurits NM, Roerdink J, JBTM. Data-driven visualization and group analysis of multichannel EEG coherence with functional units. *IEEE Trans Vis Comput Graph* 2008;14 (4), in press.

- ten Caat M, Maurits NM, Roerdink JBTM. Design and evaluation of tiled parallel coordinate visualization of multichannel EEG data. *IEEE Trans Vis Comput Graph* 2007a;13(1):70–9.
- ten Caat M, Maurits NM, Roerdink JBTM. Functional unit maps for data-driven visualization of high-density EEG coherence. In: *Proceedings of Eurographics/IEEE VGTC Symposium on Visualization (EuroVis)*; 2007b. p. 259–66.
- ten Caat M, Maurits NM, Roerdink JBTM. Watershed-based visualization of high-density EEG coherence. In: Banon GJF, Barrera J, de Mendoca Braga-Neto U, editors. *Proceedings of the 8th International Symposium on Mathematical Morphology*; 2007c. p. 289–300.
- Varela F, Lachaux JP, Rodriguez E, Martinerie J. The brainweb: phase synchronization and large-scale integration. *Nat Rev Neurosci* 2001;2(4):229–39.
- von Stein A, Sarnthein J. Different frequencies for different scales of cortical integration: from local gamma to long range alpha/theta synchronization. *Int J Psychophysiol* 2000;38:301–13.
- Watts DJ, Strogatz SH. Collective dynamics of 'small-world' networks. *Nature* 1998;393(6684):440–2.